Geochemistry
Geophysics
Geosystems
G3

Volume 14, Number 4
17 April 2013
doi:10.1002/ggge.20088
ISSN: 1525-2027

Published by AGU and the Geochemical Society

Temporal trends in vent fluid iron and sulfide chemistry following the 2005/2006 eruption at East Pacific Rise, 9°50′N

Mustafa Yücel

College of Earth, Ocean, and Environment, School of Marine Science and Policy, University of Delaware, Lewes, Delaware, 19958, USA

Now at GEOMAR – Helmholtz Centre for Ocean Research Kiel, Wischoffstr. 1–3, 24148 Kiel, Germany (myuecel@geomar.de)

George W. Luther III

College of Earth, Ocean, and Environment, School of Marine Science and Policy, University of Delaware, Lewes, Delaware, 19958, USA

[1] The chemistry of vent fluids that emanate to the seafloor undergoes dramatic changes after volcanic eruptions. Data on these changes are still limited, but the best studied example is the East Pacific Rise (EPR) at 9°50′N, where the temporal evolution of the vent fluid chemistry after the 1991/1992 eruption was documented. The area underwent another eruption sequence during late 2005/early 2006, and here we show that a similar evolution is recurring in the iron and sulfide contents of the high-temperature fluids sampled in June 2006, January 2007, and June 2008. The vents have had increasing dissolved iron and decreasing acid-volatile sulfide (free sulfide plus FeS) concentrations with 1 order of magnitude variation. In addition, chromium reducible sulfide (mainly pyrite) also had fivefold decreasing concentrations over the 3 years. Our results confirm a pattern that was noted only once before for 9°50′N EPR and emphasize the dramatic yearly variability in the concentrations of iron-sulfur species emanating from vents.

Components: 4,378 words, 2 figures, 2 tables.

Keywords: hydrothermal vents; East Pacific Rise; seafloor eruption; sulfide; iron.

Index Terms: 0450 Hydrothermal systems: Hydrothermal systems (1034, 3017, 3616, 4832, 8135, 8424); 1034 Hydrothermal systems: Hydrothermal systems (0450, 3017, 3616, 4832, 8135, 8424); 3017 Hydrothermal systems: Hydrothermal systems (0450, 1034, 3616, 4832, 8135, 8424); 3616 Hydrothermal systems: Hydrothermal systems (0450, 1034, 3017, 4832, 8135, 8424); 8135 Hydrothermal systems: Hydrothermal systems (0450, 1034, 3017, 3616, 4832, 8424); 8424 Hydrothermal systems: Hydrothermal systems (0450, 1034, 3017, 3616, 4832, 8135).

Received 22 October 2012; **Revised** 5 February 2012; **Accepted** 7 February 2013; **Published** 17 April 2013.

Yücel M. and Luther G. W. III (2013), Temporal trends in vent fluid iron and sulfide chemistry following the 2005/2006 eruption at East Pacific Rise, 9°50′N, *Geochem. Geophys. Geosyst.*, *14*, 759–765, doi:10.1002/ggge.20088.

1. Introduction

[2] The East Pacific Rise (EPR) at 9°50′N is a fast-spreading mid-ocean ridge with a spreading rate of 11 cm/yr [*Carbotte and Macdonald*, 1992] that separates the Pacific Plate from the Nazca Plate and the Cocos Plate. It is basalt hosted and therefore considered a less reducing system compared with the serpentinite-hosted systems of the Mid-Atlantic Ridge [*McCollom and Seewald*, 2007]. The EPR is also a dynamic hydrothermal system with pronounced temporal variability in fluid chemistry, mainly because of the repeated volcanic eruptions and/or dike intrusions in 1991/1992 and 2005/2006 in this region [*Fornari et al*., 2012; *Von Damm*, 2004]. These events not only changed the composition of the fluids entering the ocean but also affected the temporal succession of the productive biological communities surrounding the high-temperature vents [*Luther et al*., 2012; *Shank et al*., 1998]. This is mainly due to the fact that the availability and speciation of sulfide, where iron plays an important role, are the primary driver of the establishment of these communities [*Gartman et al*., 2011; *Luther et al*., 2001]. Therefore, since the first recorded eruption at 9°50′N EPR in 1991/1992, research efforts have concentrated on documenting the temporal evolution of the high-temperature vent fluid chemistry [*Von Damm et al*., 1995; *Von Damm*, 2000, 2004] and the chemistry of the low-temperature diffuse fluids surrounding the vents [*Le Bris et al*., 2006; *Luther et al*., 2012; *Moore et al*., 2009; *Nees et al*., 2008, 2009; *Shank et al*., 1998].

[3] In the weeks after the 1991/1992 eruption at 9°50′N EPR, the vent fluids were highly enriched in volatile chemical species and depleted in metals due to phase separation below the seafloor and the subsequent enrichment of the vapor phase in the vent fluids. With time, metal content increased in the fluids, whereas volatile content (e.g., H_2S) decreased [*Von Damm et al*., 1995; *Von Damm*, 2004], However, *Von Damm* [2004] noted annual fluctuations in Fe concentrations, including the decrease in Fe content of the Bio9 vent from 2000 to 2002. This observation underscores the need to better constrain the causes for and measured responses of temporal changes in the chemistry of hydrothermal vent fluids of 9°50′N EPR, which is particularly interesting because of its accessibility and high rate of activity [*Von Damm*, 2004].

[4] A second eruption sequence occurred at 9°50′N EPR in late 2005/early 2006 [*Cowen et al*., 2007; *Fornari et al*., 2012; *Tolstoy et al*., 2006], affecting almost all the vents that were studied previously (see Figure 1). This event created a new “time zero” and presented an opportunity to study the temporal evolution of the vent chemistry of this dynamic hydrothermal system as the chloride concentration decreased then increased as in the 1991 eruption [*Fornari et al*., 2012]. In this paper, we evaluate temporal trends from the perspective of the iron and sulfur chemistry of the high-temperature fluids in the 3 years following the 2005/2006 eruption at 9°50′N EPR. Our results for these chemical tracers allow us to compare the new eruptive cycle with the previous one and eventually confirm a trend that was noted only once before.

2. Methods

[5] We sampled the high-temperature vent fluids soon after the 2005/2006 eruption during the June 2006 NSF rapid response cruise. We revisited the region in January 2007 and June 2008. The 10 high-temperature vents studied at 9°50′N EPR are located between 9°52′N and 9°46′N (Figure 1 and Table 1). The vents sampled in each year are detailed in Table 2. Three vents (Bio, P, and L) were sampled in multiple years, enabling us to track temporal changes in their fluid chemistries.

[6] Prior to vent fluid sampling, temperature was measured with a high-temperature probe. Titanium samplers (also called “major samplers”) were used to sample high-temperature vent fluids. The nozzle of the major sampler was placed 10–15 cm inside the orifice to maximize the sampling of the actual vent fluid just before it enters the ocean. Upon retrieval of the sample, subsamples were filtered (0.2 μm) into 15 mL acid-washed polypropylene test tubes. Dissolved H_2S in the samples was fixed by adding 2 mL of unfiltered or filtered subsamples to test tubes containing 2 mL of 0.5 mL NaOH and then adding 2 mL of 0.1 M zinc acetate. The test tubes were shaken well with formation of a white precipitate, and then the fixed sample was frozen immediately at −20°C. The addition of Zn acetate causes the precipitation of free sulfide and FeS as ZnS. These samples were analyzed sequentially for their acid-volatile sulfide (AVS) and chromium reducible sulfide (CRS) contents in our shore-based laboratory. ZnS is acid volatile; therefore, AVS provides a measure of the free sulfide and FeS-sulfide contents of the vent fluid. On the other hand, CRS provides a measure of the concentrations of certain metal sulfides with disulfide linkages, such as FeS_2 (pyrite) and $CuFeS_2$ (chalcopyrite). As demonstrated by *Yücel et al*. [2011], the filtered CRS fraction was mostly composed of nanoparticle pyrite. As a result, this approach gives the speciation

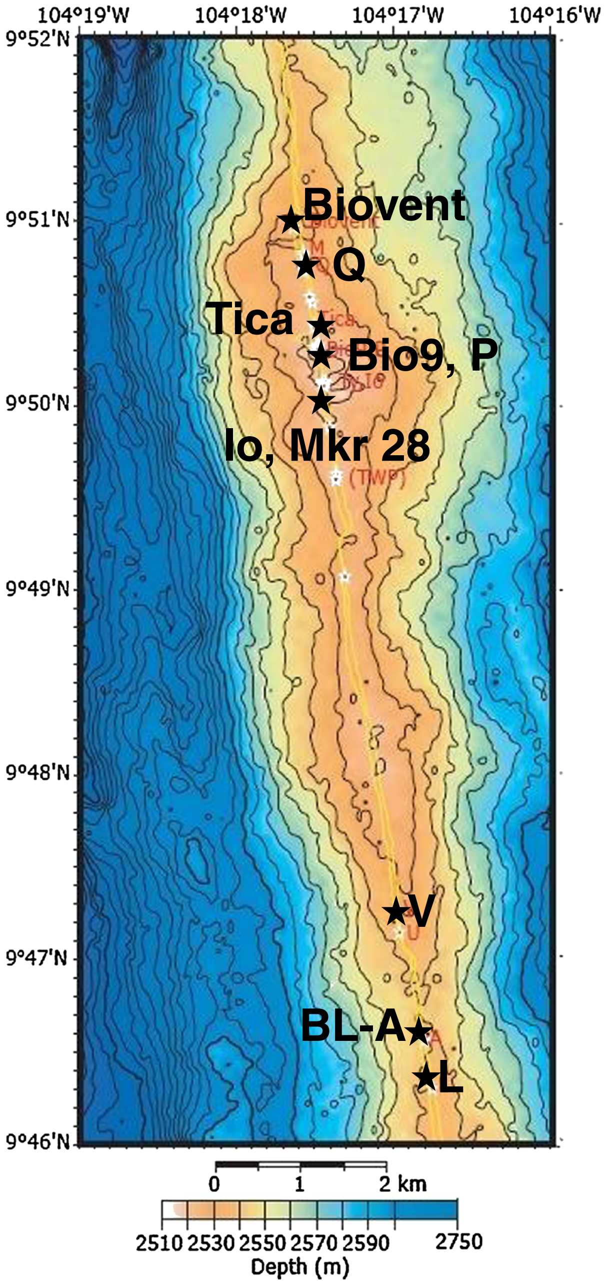

Figure 1. Locations of the studied hydrothermal vents at 9°50′N EPR. The vent field excluding the southern vents [V, L, and Bucket Lid A (BL-A)] has been studied intensively in the past decades [see *Fornari et al.*, 2012]. Map is adapted from *Von Damm* [2004].

of the reduced sulfur for the vent fluid, whereas previous work by *Von Damm* [2004] was based only on colorimetric sulfide analysis of vent fluids.

[7] The AVS-CRS sequential leaching procedure is as follows: Samples were placed in a purge-and-trap system that contained tightly closed glass reaction vessels continuously purged with ultra-high-purity argon. The gas passed through the liquid and was carried through Teflon tubing, at the end of which glass test tubes containing 20 mL of 0.1 M NaOH were placed. NaOH solution was made trace metal clean by adding excess $MgCl_2$, precipitating any metals with $Mg(OH)_2$ [*Wu and Boyle*, 1998] and removing the liquid portion. In order to recover the AVS, about 3 mL of 3 N trace metal–clean HCl was injected to each reaction vessel via a 10 mL syringe. Evolving H_2S was trapped in 20 mL of deoxygenated 0.1 N NaOH. Ninety minutes after the addition of HCl, aliquots of samples from NaOH traps were analyzed by cyclic voltammetry with a Hg drop electrode. The concentration of sulfide in the traps was used to back-calculate the concentration of AVS in the sample. After this step, acidified (in 1 M HCl) Cr(II) was added to the reaction vessel and pyrite sulfur was reduced to H_2S. Cr(II) was prepared on the day of analysis using a Jones reduction column, which consisted of amalgamated zinc particles. When 1 M $CrCl_3$ (in 1 M HCl) solution, which is green, is passed through this column, it is reduced to Cr(II), which is blue. The Cr(II) solution was immediately withdrawn from the bottom of the column with a syringe and injected [approximately 10 mL to have excess Cr(II)] to the reaction vessels. The evolving H_2S was trapped similarly in a new 0.1 N deoxygenated and trace metal–clean NaOH solution, and aliquots were analyzed by cyclic voltammetry. For the calibration of the Hg drop electrode, fresh sulfide standard was prepared by dissolving a weighed amount of solid Na_2S standard in deoxygenated deionized water. The overall detection limit of our leaching procedure for AVS and CRS was 10 μM.

[8] Dissolved iron and pH were measured on board ship on filtered samples. Ferrozine reagent was used for the colorimetric determination of dissolved iron [*Stookey*, 1970] with a portable spectrophotometer (SP 100 V, Analytical Instrument Systems, Inc.). A filtered sample (50–2000 μL; depending on the concentration of the sample) was added to a test tube containing 8 mL of deionized H_2O acidified with HCl, 1 mL of 2.5 M NH_4 acetate, and 1 mL of 0.01 M ferrozine. Fe(II) stock solution was prepared by dissolving ferrous ammonium sulfate [Mohr's salt, $(NH_4)_2(Fe)(SO_4)_2{\cdot}6H_2O$] in 1% trace metal–clean HCl (Optima). Standard solutions for the calibration of the spectrophotometer were prepared in ammonium acetate buffer as above and calibration was performed daily.

Table 1. Studied Hydrothermal Vent Locations and Water Depths

	Latitude (North)	Longitude (West)	Depth (m)
Biovent	9°50′57.75″	104°17′37.00″	2501
Q	9°50′44.73″	104°17′35.63″	2504
Tica	9°50′24.64″	104°17′30.00″	2509
Bio9	9°50′18.75″	104°17′29.03″	2509
P	9°50′16.79″	104°17′28.39″	2509
Io	9°50′6.74″	104°17′26.65″	2502
Marker 28	9°50′6.74″	104°17′26.65″	2502
V	9°47′13.83″	104°16′59.34″	2517
Bucket Lid A	9°46′30.02″	104°16′48.60″	2541
L	9°46′15.37″	104°16′44.93″	2519

3. Results and Discussion

[9] All vents sampled in 2006 (Table 2) except Bucket Lid A had temperatures higher than 300°C, with a maximum of 386°C (P vent). The lowest shipboard pH measured was 3.41 (Q vent), but the highest pH measured was 5.76 (L vent). Dissolved iron was highest with 1.43 mM in the Q vent. All samples (filtered) except the Q vent had AVS concentrations close to or above 10 mM. The Io vent had the highest AVS with 15.6 mM. Overall, the measured CRS was 1%–11% of the sum of AVS and CRS or the total reduced dissolved sulfide.

[10] In 2007, the lowest and highest pH levels measured were 2.92 in the marker 28-C sample and 5.12 in the L vent. The dissolved iron concentration was highest in the marker 28-A vent with 5.15 mM and lowest in marker 28-B with 0.493 mM. The AVS was highest in the marker 28-C sample (11.8 mM) and lowest in the L vent (0.761 mM), both measured on filtered samples. The AVS concentrations in filtered and unfiltered samples did not differ significantly. In contrast, the CRS concentration decreased dramatically upon filtering, for example, from 1.64 to 0.152 mM for the Biovent (Table 2). For filtered samples, CRS made up 2%–10% of the total reduced dissolved sulfide in the hydrothermal vent samples from January 2007.

[11] In June 2008, the highest and lowest temperatures measured were 374°C (P vent) and 300°C, respectively, for the Tica vent (Table 2). The Biovent had the lowest pH (2.98) and Tica had the highest (3.87). The highest dissolved iron concentration was 2.52 mM (P vent). The AVS concentration in filtered samples was highest in Tica with 2.65 mM and lowest in Bio9 with 1.2 mM. In the filtered samples, CRS made up 2%–5% of the total dissolved reduced sulfide, similar to the results from 2006 and 2007.

Table 2. Results of the Temperature, pH, Iron, AVS, and CRS Measurements on the Vent Fluids of 9°50′N EPR

Dive no.	Vent	Temperature (°C)	pH	$[Fe^{2+}]$ (mM)	AVS-filtered Fraction (mM)	AVS-unfiltered Fraction (mM)	CRS-filtered Fraction (mM)	CRS-unfiltered Fraction (mM)
				June 2006				
4202	Q	318	3.41	1.43	4.17 ± 0.09	n.m.	0.529 ± 0.112	n.m.
4203	P	386	3.63	0.665	12.3 ± 1.5	n.m.	0.81 ± 0.09	n.m.
4205	BL-A	270	4.8	0.075	14.7 ± 0.1	n.m.	0.136 ± 0.03	n.m.
4205	L	346	5.76	0.0081	9.56	n.m.	0.303	n.m.
4205	V	319	4.66	0.0084	12.8	n.m.	0.655	n.m.
4207	Io	375	3.56	0.198	15.6 ±1.2	n.m.	0.624 ± 0.06	n.m.
				January 2007				
4306	Biovent	306	3.3	0.777	4.13 ± 0.08	4.7 ± 0.5	0.152 ± 0.027	1.64 ± 0.12
4307	L	n.m.	5.12	1.31	0.761 ± 0.045	0.637 ± 0.026	0.08 ± 0.03	0.47 ± 0.14
4314	Mkr 28-A	n.m.	3.04	5.15	6.82 ± 0.24	8.07 ± 0.28	0.237 ± 0.131	0.429 ± 0.13
4314	Mkr 28-B	n.m.	3.84	0.493	3.45 ± 0.06	4.3 ± 0.5	0.085 ± 0.023	0.612 ± 0.368
4314	Mkr 28-C	n.m.	2.92	1.71	11.8 ± 0.1	11.5 ± 0.3	0.330 ± 0.05	0.414 ± 0.001
				June 2008				
4403	P	374	3.3	2.52	1.95 ± 0.17	2.09 ± 0.34	0.053 ± 0.01	0.161 ± 0.009
4403	Tica	300	3.87	0.164	2.65 ± 0.29	2.42 ± 0.21	0.064 ± 0.032	0.110 ± 0.095
4405	Bio9	360	3.36	1.2	1.10 ± 0.09	1.20 ± 0.19	0.054 ± 0.002	0.368 ± 0.181
4407	Biovent	350	2.98	2.15	2.49 ±0.43	2.42 ± 0.23	0.088 ± 0.004	0.211 ± 0.042

The standard errors associated with AVS and CRS are based on triplicate measurements. The error in iron measurements was less than 1%. BL-A stands for Bucket Lid A vent; Mkr, marker.

n.m. : not measured.

[12] Our results indicate that the subseafloor volcanic processes that caused the eruption at EPR in 2005/2006 led to the phase separation of the vent fluids, resulting in the initial enrichment of emitted volatiles in them. As a result, the most notable temporal change in the EPR data set from 2006 to 2008 is the decline in dissolved sulfide (AVS and CRS) concentrations over the 3 years following 2005/2006 with increasing Fe(II) (Figure 2). In June 2006, about 4–8 months after the eruption, the average AVS of the six vents was 11.7 mM, with an average dissolved iron concentration of 0.382 mM. The average AVS decreased by 50% to 5.4 mM in 2007 and by another 50% to 2.05 mM in 2008. CRS also decreased from an average of 0.51 mM (2006) to 0.178 mM in 2007 and to 0.065 mM in 2008. The average dissolved iron increased by 5-fold to 1.89 mM in 2007 and decreased slightly to 1.51 mM in 2008. There was no significant temporal change in either the pH or the temperature. Among the vents with multiyear data, the most dramatic changes are that sulfide in the P vent decreased by 6-fold over 2 years, whereas that in the L vent decreased by 10-fold over 1 year.

[13] After the 1991 eruption at 9°50′N EPR, *Von Damm et al.* [1995] also observed elevated sulfide concentrations in the newly formed vents. They sampled the vents within 1 month after the eruption and calculated end-member H_2S concentrations as high as 71 mmol kg^{-1} with measured temperatures as high as 403°C. They did not report the actual measured values, so a direct comparison of our data with theirs is not possible. Still, their data showed a sixfold decrease in maximum sulfide concentrations (71 to 11 mM kg^{-1}) from 1991 to 1994. *Von Damm* [2004] provided a more complete set of observations with actual measured values for the 5 years following the 1991 eruption in the 9°50′N EPR vents. These observations included data on two vents: P and Bio9. In the 4 years following the 1991 eruption, the Bio9 vent sulfide concentration decreased by fivefold from 21 to 4 mM and the P vent sulfide decreased by eightfold from 25 to 2 mM. The iron concentrations fluctuated in the period 1991–1994 between 2.19 and 1.06 mM for the Bio9 vent as well as between 0.064 and 5.78 mM for the P vent, similar to our 2007 and 2008 data, and the concentrations kept increasing until 1996, reaching values exceeding 8 mM. These observations after the 1991 eruption are consistent with our study for the 3 years following the 2005/2006 eruption, indicative of initial phase separation, where vent fluids were dominated by a H_2S-laden vapor phase. With the gradual lessening of the volatiles and increasing presence of the brine phase, the vent fluids are gradually enriched in metals such as iron.

[14] The picture that emerged after the documentation of two eruptive cycles at 9°50′N EPR is consistent with the available results on other vent systems, although those data are mostly on diffuse fluids [*Butterfield et al.*, 1997, 2004]. For example, after the 1993 eruption in the CoAxial segment of the Juan de Fuca Ridge, the diffuse flow (<50°C) fluids displayed initial elevation in sulfide concentrations (max. 0.38 mM) in the weeks after the

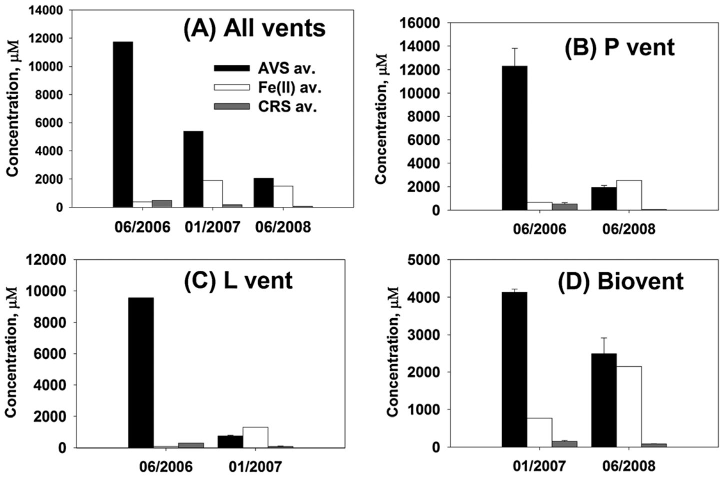

Figure 2. Temporal changes in the EPR vents through 2006 to 2008. (a) Averages of all measured AVS, CRS, and dissolved Fe concentrations are plotted to obtain general trends. (b) Temporal change in the chemistry of the P vent from 2006 to 2008. (c) Temporal change in the chemistry of the L vent from 2006 to 2007. (d) Temporal change in the chemistry of the Biovent from 2007 to 2008.

event, followed by a gradual decline in sulfide and an increase in iron (max. 0.058 mM) over 2 years [*Butterfield et al*., 1997]. One contrasting feature was the complete disappearance of sulfide after several years in the vent fluids of the CoAxial site. Although a disappearance of sulfide was not observed either in high temperature [*Von Damm*, 2004; this study] or in low-temperature diffuse fluids [*Luther et al*., 2012; *Nees et al*., 2009] at 9°50′ EPR, similar decreases in sulfide and increases in iron occurred. These data underline the specific dynamics of each vent system and indicate that the chemical compositions of the vent fluids on the global mid-ocean ridge are usually evolving. Thus, it is difficult to speak of stable concentration levels over several years, at least for iron-sulfide species.

[15] In the context of the importance of vent-derived iron input for ocean biogeochemistry, our findings raise the question of what the consequences of these dramatic yearly changes in the iron concentrations to the ocean from vents are. Our iron data indicate that in the post-eruptive period, the averages of all vent concentrations can vary by 5-fold, whereas individual vents can differ by as much as 15-fold in iron concentrations (L vent). Recent research recognized that not all of the discharged iron precipitates near the vents. Instead, processes such as nanoparticle pyrite formation [*Yücel et al*., 2011] and organic complexation [*Bennett et al*., 2008] are important agents in transporting vent-derived iron away from venting areas, which could in turn support primary production elsewhere. In this respect, the changing speciation of Fe-S species with time can have consequences. We have not measured the nanoparticle pyrite fraction through nitric acid digestion as done by *Yücel et al*. [2011], but based on a stoichiometric ratio of 2:1 for CRS to pyrite iron, we can estimate that up to 50% of dissolved iron could have been CRS bound in the immediate post-eruptive period (2006), whereas these fractions were about 10% in 2007 and 2008. It is possible that seafloor volcanic activity can induce orders of magnitude elevated mass fluxes and larger hydrothermal plumes than usual [*Baker*, 1995; *Baker et al*., 2012]. Under these circumstances, volcanic activity may result in a higher CRS-bound iron flux even though the concentration itself may be lower. As a consequence, in future studies, it may be worthwhile to explore the consequences of the short-term (yearly) variability in hydrothermal iron-sulfur speciation and fluxes on the ocean biogeochemistry.

4. Conclusions

[16] Hydrothermal vents at 9°50′N EPR have had increasing dissolved iron and decreasing sulfide (AVS) concentrations since the eruption that occurred in late 2005/early 2006. Phase separation–induced volatile enrichment in the subseafloor is the primary reason for unusual enrichments of the vent fluid in sulfide and high sulfide to iron ratios within 4–8 months after the eruption. Our results confirm a pattern that was noted only once before for the 9°50′N EPR and emphasize the dramatic yearly variability in the concentrations of iron-sulfur species emanating from vents, a dynamic phenomenon that may affect iron biogeochemical cycling in the overlying waters.

Acknowledgments

[17] This work was supported by the National Science Foundation under Grants OCE-0308398, OCE-0326434, and OCE-1131109. We thank the DSV *Alvin* group for their patience and support, including pre-cruise and post-cruise planning as well as performing detailed manipulations to collect the data.

References

Baker, E. T. (1995), Characteristics of hydrothermal discharge following a magmatic intrusion, *Geol. Soc. London, Special Publ.*, *87*(1), 65–76, doi:10.1144/GSL.SP.1995.087.01.06.

Baker, E. T., W. W. Chadwick Jr., J. P. Cowen, R. P. Dziak, K. H. Rubin, and D. J. Fornari (2012), Hydrothermal discharge during submarine eruptions: The importance of detection, response, and new technology, *Oceanogr.*, *25*(1), 128–141, http://dx.doi.org/10.5670/oceanog.2012.11.

Bennett, S. A., E. P. Achterberg, D. P. Connelly, P. J. Statham, G. R. Fones, and C. R. German (2008), The distribution and stabilization of dissolved Fe in deep-sea hydrothermal plumes, *Earth Planet. Sci. Lett.*, *270*, 157–167, doi:10.1016/j.epsl.2008.01.048.

Butterfield, D. A., I. R. Jonasson, G. J. Massoth, R. A. Feely, K. K. Roe, R. E. Embley, J. F. Holden, R. E. McDuff, M. D. Lilley, and J. R. Delaney (1997), Seafloor eruptions and evolution of hydrothermal fluid chemistry, *Phil. Trans. R. Soc. Lond. A*, *355*, 369–386, doi:10.1098/rsta.1997.0013.

Butterfield, D. A., K. K. Roe, M. D. Lilley, J. A. Huber, J. A. Baross, R. W. Embley, and G. J. Massoth (2004), Mixing, reaction and microbial activity in sub-seafloor revealed by temporal and spatial variation in diffuse flow vents at Axial Volcano, in The Subseafloor Biosphere at Mid-Ocean Ridges, edited by W. S. D. Wilcock, E. F. DeLong, D. S. Kelley, J. A. Baross, and S. C. Cary, pp. 269–289, Geophys. Monogr. Ser., Vol. 144, AGU, Washington, D. C., doi:10.1029/GM144.

Carbotte, S., and K. Macdonald (1992), East Pacific Rise 8°-10°30’N: Evolution of ridge segments and discontinuities from SeaMARC II and three-dimensional magnetic studies, *J. Geophys. Res.*, *97*, 6959–6982, doi:10.1029/91JB03065.

Cowen, J. P., et al. (2007), Volcanic eruptions at East Pacific Rise near 9°50'N, *Eos, Trans., Am. Geophys. Union*, *88*, 81–92, doi:10.1029/2007EO070001.

Fornari, D. J., et al. (2012), The East Pacific Rise between 9°N and 10°N: Twenty-five years of integrated, multidisciplinary oceanic spreading center studies, *Oceanogr.*, *25*(1):18–43, doi:10.5670/oceanog.2012.02.

Gartman, A., M. Yücel, A. S. Madison, D. W. Chu, S. Ma, C. P. Janzen, E. L. Becker, R. A. Beinart, P. R. Girguis, and G. W. Luther (2011), Sulfide oxidation across diffuse flow zones of hydrothermal vents, *Aquat. Geochem.*, *17*, 583–601, doi:10.1007/s10498-011-9136-1.

Le Bris, N., B. Govenar, C. Le Gall, and C. R. Fisher (2006), Variability of physico-chemical conditions in 9º50'N EPR diffuse flow vent habitats, *Mar. Chem.*, *98*, 167–182, doi:10.1016/j.marchem.2005.08.008.

Luther III, G. W., T. F. Rozan, M. Taillefert, D. B. Nuzzio, T. M. Shank, R. A. Lutz, S. C. Cary, and C. Di Meo (2001), Chemical speciation drives hydrothermal vent ecology, *Nature*, *410*, 813–816, doi:10.1038/35071069.

Luther III, G. W., et al. (2012), Chemistry, temperature, and faunal distributions at diffuse-flow hydrothermal vents: Comparison of two geologically distinct ridge systems, *Oceanogr.*, *25*(1), 234–245, doi:10.5670/oceanog.2012.22.

McCollom, T. M., and J. S. Seewald (2007), Abiotic synthesis of organic compounds in deep-sea hydrothermal environments, *Chem. Rev.*, *107*, 382–401, doi:10.1002/chin.200720264.

Nees H. A., et al. (2008), Hydrothermal vent mussel habitat chemistry, pre- and post-eruption at 9°50' north on the East Pacific Rise, *J. Shellfish Res.*, *27*, 169–175, doi:10.2983/0730-8000(2008)27[169:HVMHCP]2.0.CO;2.

Nees, H. A., R. A. Lutz, T. M. Shank, and G. W. Luther III (2009), Pre- and post-eruption diffuse flow variability among tubeworm habitats at 9 degrees 50' north on the East Pacific Rise, *Deep-Sea Res. Part II*, *56*, 1607–1615, doi:10.1016/j.dsr2.2009.05.007.

Moore, T. S., T. M. Shank, D. B. Nuzzio, and G. W. Luther III (2009), Time-series chemical and temperature habitat characterization of diffuse flow hydrothermal sites at 9 degrees 50' N East Pacific Rise, *Deep-Sea Res. Part II*, *56*, 1616–1621, doi:10.1016/j.dsr2.2009.05.008.

Shank, T. M., D. J. Fornari, K. L. Von Damm, M. D. Lilley, R. M. Haymon, and R. A. Lutz (1998), Temporal and spatial patterns of biological community development at nascent deep-sea hydrothermal vents (9°50'N, East Pacific Rise), *Deep-Sea Res. Part II*, *45*, 465–515, doi:10.1016/S0967-0645(97)00089-1.

Stookey, L. L. (1970), Ferrozine – A new spectrophotometric reagent for iron, *Anal. Chem.*, *42*, 779–781, doi:10.1021/ac60289a016.

Tolstoy, M., et al. (2006), A sea-floor spreading event captured by seismometers, *Science*, *314*, 1920–1922, doi:10.1126/science.1133950.

Von Damm, K. L. (2000), Chemistry of hydrothermal vent fluids from 9-10 N, East Pacific Rise: "Time zero," the immediate post eruptive period, *J. Geophys. Res.*, *105*, 203–222, doi:10.1029/1999JB900414.

Von Damm, K. L., S. E. Oosting, R. Kozlowski, L. G. Buttermore, D. C. Colodner, H. N. Edmonds, J. M. Edmond, and J. M. Grebmeier (1995), Evolution of East Pacific Rise hydrothermal vent fluids following a volcanic eruption, *Nature*, *375*, 47–50, doi:10.1038/375047a0.

Von Damm, K. L. (2004), Evolution of the hydrothermal system at East Pacific Rise, 9°50'N: geochemical evidence for changes in the upper oceanic crust, in Mid-Ocean Ridges: Hydrothermal Interactions Between the Lithosphere and Oceans, Geophys. Monogr. Ser., *148*, edited by C. R. German, J. Lin, L. M. Parson, pp. 285–304, AGU, Washington, D.C., doi:10.1029/148GM12.

Wu, J., and E. A. Boyle (1998), Determination of iron in seawater by high resolution isotope dilution inductively coupled plasma mass spectrometry after $Mg(OH)_2$ coprecipitation, *Anal. Chim. Acta*, *367*, 183–191, doi:10.1016/S0003-2670(98)00145-7.

Yücel, M., A. Gartman, C. S. Chan, and G. W. Luther (2011), Hydrothermal vents as a kinetically stable source of iron-sulphide-bearing nanoparticles to the ocean, *Nat. Geosci.*, *4*, 367–371, doi:10.1038/ngeo1148.